Title

Delayed Repolarization Underlies Ventricular Arrhythmias in Rats With Heart Failure and Preserved Ejection Fraction

Journal

Circulation, 136(21)

ISSN

0009-7322

Authors

Cho, Jae Hyung
Zhang, Rui
Kilfoil, Peter J
et al.

Publication Date

2017-11-21

DOI

10.1161/circulationaha.117.028202

Peer reviewed

HHS Public Access

Author manuscript

Circulation. Author manuscript; available in PMC 2018 November 21.

Published in final edited form as:

Circulation. 2017 November 21; 136(21): 2037–2050. doi:10.1161/CIRCULATIONAHA.117.028202.

Delayed Repolarization Underlies Ventricular Arrhythmias in Rats with Heart Failure and Preserved Ejection Fraction

Jae Hyung Cho, MD[1], **Rui Zhang, MD**[1], **Peter J. Kilfoil, PhD**[1], **Romain Gallet, MD**[2], **Geoffrey de Couto, PhD**[1], **Catherine Bresee, MS**[3], **Joshua I. Goldhaber, MD**[1], **Eduardo Marbán, MD, PhD**[1], and **Eugenio Cingolani, MD**[1]

[1]Cedars-Sinai Heart Institute, Los Angeles, CA, USA, Twitter handle: @bluemed78 (Jae Hyung Cho, MD)

[2]Henri Mondor University Hospital, Créteil, France

[3]Biostatistics and Bioinformatics Research Center, Cedars-Sinai Medical Center, CA, USA

Abstract

Background—Heart failure with preserved ejection fraction (HFpEF) represents approximately half of heart failure, and its incidence continues to increase. The leading cause of mortality in HFpEF is sudden death, but little is known about the underlying mechanisms.

Methods—Dahl salt-sensitive rats were fed a high-salt diet (8% NaCl) from 7 weeks of age to induce HFpEF (n=38). Rats fed a normal-salt diet (0.3% NaCl) served as controls (n=13). Echocardiograms were performed to assess systolic and diastolic function from 14 weeks of age. HFpEF-verified and control rats underwent programmed electrical stimulation (PES). QTc interval was measured by surface electrocardiography (ECG). The mechanisms of ventricular arrhythmias (VA) were probed by optical mapping, whole-cell patch clamp to measure action potential duration and ionic currents, and quantitative polymerase chain reaction and western blotting to investigate changes in ion channel expression.

Results—After 7 weeks of high-salt diet, 31 of 38 rats showed diastolic dysfunction and preserved ejection fraction along with signs of heart failure, hence diagnosed with HFpEF. PES demonstrated increased susceptibility to VA in HFpEF rats ($p < 0.001$ vs. controls). The arrhythmogenicity index was increased ($p < 0.001$), and the QTc interval on ECG was prolonged ($p < 0.001$) in HFpEF rats. Optical mapping of HFpEF hearts demonstrated prolonged action

Correspondence: Eduardo Marbán, MD, PhD, Cedars-Sinai Heart Institute, 8700 Beverly Blvd, Los Angeles, CA 90048, Phone: 310.423.7557, Fax: 310.423.7637, Eduardo.Marban@csmc.edu; Eugenio Cingolani, MD, Cedars-Sinai Heart Institute, 127 S. San Vicente Blvd, Los Angeles, CA 90048, Phone: 310.248.6679, Fax: 310.423.6795, Eugenio.Cingolani@csmc.edu.

DISCLOSURES

JHC - None
RZ - None
PJK - None
RG - None
GdC – None
CB - None
JIG - None
EM - None
EC - None

potentials ($p < 0.05$) and multiple re-entry circuits during induced VA. Single-cell recordings of cardiomyocytes isolated from HFpEF rats confirmed a delay of repolarization ($p=0.001$) and revealed down-regulation of transient outward potassium current (I_{to}) ($p < 0.05$). The rapid component of the delayed rectifier potassium current (I_{Kr}), and the inward rectifier potassium current (I_{K1}), were also down-regulated ($p < 0.05$), but the current densities were much lower than for I_{to}. In accordance with the reduction of I_{to}, both *Kcnd3* transcript and Kv4.3 protein levels were decreased in HFpEF rat hearts.

Conclusions—Susceptibility to VA was markedly increased in rats with HFpEF. Underlying abnormalities include QTc prolongation, delayed repolarization from down-regulation of potassium currents, and multiple re-entry circuits during VA. Our findings are consistent with the hypothesis that potassium current down-regulation leads to abnormal repolarization in HFpEF, which in turn predisposes to VA and sudden cardiac death.

Keywords

Heart Failure; Heart Failure with Preserved Ejection Fraction; Arrhythmia; Ventricular Arrhythmia; Ventricular Tachycardia; Ventricular Fibrillation; Action Potential; Action Potential Prolongation; Potassium Current; Transient Outward Potassium Current; Optical Mapping; Patch Clmap; Fibrosis

INTRODUCTION

Heart disease is the leading cause of death in the United States, with coronary artery disease and heart failure (HF) being the leading contributing conditions.[1] Disability and frequent hospitalizations are hallmarks of the disease.[2–4] Most of the diagnostic and therapeutic advances in the last two decades have been primarily in HF with reduced ejection fraction (HFrEF), which has been classically seen as the most common type of HF.[2, 3] The diastolic counterpart, heart failure with preserved ejection fraction (HFpEF), has been steadily increasing due to an aging population with frequent hypertension and obesity, such that HFpEF now accounts for ~half (39–72%) of all HF patients.[5–7] Abnormal cardiac relaxation is a hallmark of HFpEF, but the underlying mechanisms remain unclear.[6, 8] Sudden cardiac death (SCD) is the most common cause of death in HF, comprising approximately 50% of the death in HFrEF and ~25% in HFpEF.[9–13] Most SCD in HF patients is likely secondary to ventricular arrhythmias (VA), although this conjecture is more secure for HFrEF than for HFpEF.[9, 10, 13] Action potential prolongation, down-regulation of outward potassium currents, and altered calcium handling are important contributors to HFrEF-related VA,[9, 10, 13–16] but little is known about the electrophysiological features of HFpEF.[9, 10, 13, 14, 17] Unlike HFrEF, where numerous pharmacologic and device-based treatment options are available, no treatments have proven to be effective in improving survival in patients afflicted with HFpEF.[18–20] Here, we implemented a rodent model of HFpEF to investigate the incidence and underlying mechanisms of VA in HFpEF using *in vivo*, *ex vivo*, and single cell electrophysiology studies.

METHODS

Animal model of HFpEF

All animal experiments were approved by the Cedars-Sinai Institutional Animal Care and Use Committee (IACUC). A Dahl salt-sensitive (DSS) rat model of HFpEF was implemented as described[21–23] and as shown schematically in Fig. 1A. In brief, male 7 week-old DSS rats (Charles River Laboratories, MA) underwent baseline transthoracic echocardiography and were then randomly assigned to a high-salt (HS) diet (AIN-76A + 8% NaCl with irradiation, Research Diets, NJ) to induce HFpEF (n=38),[21, 22] or to a normal-salt (NS) diet (AIN-76A [0.3 % NaCl] with irradiation) as controls (n=13). Feeding was continued ad libitum until rats reached the experimental endpoints at 14–18 weeks old. Transthoracic echocardiogram was repeated to measure systolic and diastolic function at 14 and 18 weeks. Most HS-fed rats showed signs of HF including weakness, decreased activity, cachexia, labored breathing, and body edema beginning at 14 weeks of age. Symptomatic HS rats demonstrating diastolic dysfunction (and preserved systolic function) by echocardiography were diagnosed with HFpEF. HS rats which failed to meet these criteria (~20% of cases) were euthanized and omitted from analysis.

Transthoracic echocardiogram

Rats were anesthetized with 5% isoflurane (induction) and maintained with 2% isoflurane for transthoracic echocardiography (Vevo 770, VisualSonics, Toronto, Canada). Systolic function was evaluated by calculating ejection fraction (%) from images obtained in the parasternal short axis view as described.[24] Diastolic function was assessed from the apical four chamber view by measuring E/A and E/E' ratios.[21–24] E wave (early filling) and A wave (atrial filling) were measured by pulse wave Doppler mode between the tips of the mitral valve.[21–24] E' and A' waves were measured with tissue Doppler mode at the septal corner of the mitral annulus (the junction between the anterior mitral leaflet and ventricular septum).[24] Three separate measurements from each animal were averaged to quantify systolic and diastolic function.

Surface electrocardiogram

Surface electrocardiogram (ECG) was recorded prior to *in vivo* arrhythmia induction studies for HFpEF and control rats at 14 and 18 weeks (Dual bio-amps, AD Instruments, Dunedin, New Zealand). PR interval, QRS duration, QT interval, and RR interval were measured three times and averaged on LabChart 7 software (AD instruments, Dunedin, New Zealand). Corrected QT (QTc) interval was calculated as QT interval (ms) divided by the square root of RR interval (s).[25]

In vivo arrhythmia induction study

Animals were anesthetized with 5% isoflurane (induction), intubated, and placed on mechanical ventilation as previously described.[26] Anesthesia was maintained with 2% isoflurane during programmed electrical stimulation (PES). Core body temperature was monitored using a rectal probe and maintained at 36–38 °C via a heating lamp. ECG was monitored during the procedure (Dual bio-amps, AD Instruments, Dunedin, New Zealand).

Under general anesthesia, a mini-thoracotomy was performed to expose the apex of the heart. Following opening of the pericardial sac, a platinum electrode was placed into the apex of the left ventricle. PES was performed using an electronic stimulator (PowerLab, AD Instruments, Dunedin, New Zealand) to apply a standard PES protocol.[27–30] A drive train of 10 stimuli of S1 (5V, 1 ms pulse width, and 100 ms interval) was delivered, followed by an extra stimulus (S2) (5V and 1 ms pulse width) starting at a coupling interval of 80 ms and by 1 ms decrements until reaching the effective refractory period (ERP). If ventricular tachycardia or fibrillation were not induced, a second extra stimulus (S3) was introduced from 80 ms at progressively decremental coupling intervals until ERP was reached. Finally, a third extra stimulus (S4) was introduced from an 80 ms coupling interval until ERP was reached. If the rat failed to develop VA with three extra stimuli (S1-S2-S3-S4), the animal was deemed non-inducible. In rats that developed VA during PES, the protocol was repeated to confirm the reproducibility of the arrhythmia. To quantify the inducibility of VA, we created and implemented an arrhythmogenicity index (AI) defined by the following equation:

$$\mathbf{AI}=\frac{\text{number of VA beats}+(\text{last extra stimuli coupling interval}[\text{ms}]-40)}{\sqrt{\text{number of extra stimuli}}}$$

This index takes into account not only the duration of the arrhythmia (in number of beats), but also the aggressiveness of the PES protocol, thus allowing for a more accurate quantification of arrhythmia inducibility in both groups. Cesium chloride and magnesium sulfate were used to provoke and treat VA in control and HFpEF rats. Cesium chloride (10 ml of 1 mM) was delivered through tail vein to prolong QTc interval and provoke VA. Magnesium sulfate (1 ml of 100 mg, 0.83 M) was delivered through tail vein as well to treat VA in HFpEF rats. NS5806 (1 ml of 1 mM, Sigma-Aldrich) was delivered through tail vein to shorten QTc by activating transient outward potassium current in HFpEF rats.

Ex vivo optical mapping

For *ex vivo* optical mapping experiments, rats were anesthetized with 5% isoflurane, the chest was opened and the heart was harvested as described.[31–33] The ascending aorta was cannulated and retrogradely perfused in a Langendorff system with Tyrode's solution containing 1.8 mM $CaCl_2$ at 10 ml/min. RH237 (Molecular Probes, OR) was used to measure membrane potential changes (0.05 mg in 50 ml Tyrode's solution for 5 minutes). Blebbistatin (Sigma-Aldrich, MO) was used to as an uncoupler to avoid motion artifacts (0.5 mg in 100 ml Tyrode's solution perfusion for 10 minutes, 0.017 mM). Images were acquired using a MiCAM05 Ultima-L CMOS camera (SciMedia, CA) with filters (excitation 520/35 nm, dichroic 560 nm, emission 715 nm long-pass) and stored for offline analysis. BV-Ana software (SciMedia, CA) was used to calculate action potential duration 90 (APD90) and visualized the re-entry circuits after *ex vivo* PES.[33–37]

Isolation of cardiomyocytes

Adult ventricular cardiomyocytes were isolated as described.[38] In brief, heparin (4,000 IU per kg) was injected intraperitoneally one hour prior to excising the heart. Rats were

euthanized, and the heart was rapidly removed after thoracotomy. After cannulation of the ascending aorta, hearts were retrogadely perfused with Ca-free Tyrode's solution (NaCl 136 mM, KCl 5.4 mM, NaH_2PO_4 0.33 mM, $MgCl_2$ 1.0 mM, HEPES 10 mM, and glucose 10 mM) at a temperature of 37°C using a Langendorff apparatus. After 5 minutes of perfusion with Ca-free Tyrode's solution, an enzyme solution containing type II collagenase (1.66 mg/ml, Worthington Biomedical, Lakewood, NJ) and type XIV protease (0.13 mg/ml, Sigma-Aldrich, St. Louis, MO) in Ca-free Tyrode's solution was perfused for 20 minutes. Following enzymatic digestion, hearts were perfused with Tyrode's solution containing 0.2 mM $CaCl_2$ for 5 minutes. The left ventricle was excised, minced and filtered (100 μm) to isolate single cardiomyocytes. Calcium was re-introduced to suspend cells by gradual increases to a final concentration of 1.0 mM.

Action potential recordings

Action potentials were recorded in HFpEF and control cardiomyocytes. For action potential recordings, we placed the isolated cardiomyocytes in an experimental chamber (0.5 ml) mounted on the stage of a Nikon Diaphot inverted microscope modified for simultaneous electrophysiology and fluorescence recording. A heated bath solution (26 °C) continuously perfused the chamber. Patch electrodes were pulled from borosilicate glass (model TW150F-3, World Precision Instruments, Sarasota, FL) on a horizontal puller (model P-97, Sutter Instruments, Novato, CA). The fire-polished electrodes had a tip diameter of 2–3 μm and a resistance of 1–2 MΩ. We used an Axopatch 200B patch clamp amplifier (Molecular Devices, Sunnyvale, CA) under the control of pClamp 10 software (Molecular Devices) and a Digidata 1440A PC interface (Molecular Devices). We measured induced action potentials with the whole-cell current clamp mode. We used Tyrode's solution with 1.0 mM $CaCl_2$ as bath solution. The internal solution contained (in mM): NaCl 10, KCl 130, HEPES 10, MgATP 5, phosphocreatine 5, cAMP 0.05, and $MgCl_2$ 1; pH adjusted to 7.2 with KOH.

Transient outward potassium current

Transient outward potassium current (I_{to}) was measured using the whole-cell clamp configuration in HFpEF and control cardiomyocytes. The external solution contained (in mM): NaCl 136, KCl 5.4, NaH_2PO_4 0.33, $MgCl_2$ 1.0, HEPES 10, glucose 10, $CaCl_2$ 1.0, and nifedipine 20 μM. Final pH was adjusted to 7.4 by NaOH. The pipette solution contained: NaCl 5.4 mM, KCl 130 mM, $MgCl_2$ 1 mM, HEPES 10 mM, cAMP 0.05 mM, MgATP 5 mM, and phosphcreatine 2.8 mM, adjusted to a final pH of 7.2 by KOH. A 100 ms pre-pulse to −40 mV from a holding potential of −80 mV was used to inactivate Na^+ current and nifedipine (20 μM) to block L-type Ca current. Outward potassium currents were evoked by voltage steps to potentials from −60 mV to +60 mV in 10 mV increments lasting 3000 ms. Series resistance compensation (40% to 70%) was used. Membrane currents sampled at 5 kHz were filtered at 2 kHz. I_{to} amplitude was measured as the difference between the peak outward current and the current at the end of the pulse.[39, 40] Current density (pA/pF) was calculated from the current amplitude (pA) divided by the membrane capacitance (pF).

Rapid component of delayed rectifier potassium current

The rapid component delayed rectifier (I_{Kr}) was measured in control and HFpEF rats. The external and pipette solutions were the same as used to record I_{to}, with nifedipine (20 μM) added to block L-type Ca current. After a 100 ms pre-pulse to −40 mV to inactivate Na^+ channels, I_{Kr} was evoked by voltage steps to potentials from −60 mV to +60 mV in 10 mV increments lasting 3000 ms. I_{Kr} was defined as E-4031 sensitive current. E-4031 (1 μM, Sigma-Aldrich, MO) was applied and currents were subtracted to calculate E-4031 sensitive current (taken as I_{Kr}).

Inward rectifier potassium current

Inward rectifier potassium current (I_{K1}) was measured in control and HFpEF cardiomyocytes. The external and pipette solutions were the same as I_{to}, with nifedipine (20 μM) added to block L-type Ca current. After a 100 ms pre-pulse to −40 mV to inactivate Na^+ channels, I_{K1} was evoked by voltage steps to potentials from −120 mV to +10 mV in 10 mV increments lasting 500 ms. Barium (100 μM) was then added to the external solution; I_{K1} was defined as barium-sensitive current.

L-type calcium current

L-type calcium current (I_{CaL}) was measured in control and HFpEF cardiomyocytes. The external solution contained (in mM): NaCl 136, CsCl 20, $MgCl_2$ 0.33, HEPES 10, glucose 10, $CaCl_2$ 1.0, and tetrodotoxin 0.01. The pipette solution contained (in mM): NaCl 10, CsCl 130, $MgCl_2$ 0.33, HEPES 10, cAMP 0.05, MgATP 4, and tetraethylammonium chloride 20. I_{CaL} current was evoked by applying a 1 s voltage pre-pulse from −80 mV to −50 mV to inactivate Na channel followed by a 200 ms test pulse to 0 mV.

Quantitative reverse transcriptase polymerase chain reaction

Heart tissue was stored in Allprotect Tissue Reagent (Qiagen, Hilden, Germany) for quantitative reverse transcriptase polymerase chain reaction (RT Q-PCR). Total RNA was isolated from heart tissue using RNeasy Plus Universal Mini Kit (Qiagen, Hilden, Germany). cDNA was synthesized with 2 μg of RNA using High Capacity RNA-to-cDNA Kit (Applied Biosystems, MA). Primers were obtained from Abcam (Cambridge, UK) (*Scn5a, Cacna1c, Cacna1d, Kcnd2, Kcnd3, Kcna4, Kcna5, Kcnh2, Kcnq1, Kcnj2 and Ldha*). RT Q-PCR was performed using TaqMan Universal Master Mix II with UNG (Applied Biosystems, MA) under the following conditions: 50°C for 2 minutes (UNG incubation), 95°C for 10 minutes (polymerase activation) and 40 cycles of 95°C for 15 seconds (denaturation) and 60°C for 1 minute (annealing and extension). Each cycle threshold (CT) value was normalized to the CT value of *Ldha* (lactate dehydrogenase A). Fold change was calculated with $\hat{2}$(-ddCT) compared to the control group. Log scale of fold change was used to compare expression levels.

Protein isolation and western blot

Protein was extracted from heart tissue using Tissue Ruptor (Qiagen, Hilden, Germany) with RIPA buffer and protease inhibitor (Thermo Fisher Scientific, MA). Protein quantification was performed using Bradford Protein Assay (Bio-Rad, CA). Western blot was performed

using the NuPAGE system (4–12% Bis-Tris gradient gel, MES [2-morpholinoethane] SDS [sodium dodecyl sulfate] running buffer, transfer buffer and TBS [Tris buffered saline] Tween buffer) (Life Technologies, CA). Kv4.2, Kv4.3, Kv1.4, Kv11.1, Kir2.1 and GAPDH antibodies were obtained from Abcam (Cambridge, UK), (Kv4.2-ab16719, Kv4.3-ab99045, Kv1.4-ab16718, Kv11.1-ab92513, Kir2.1-ab109750, GAPDH-ab9483). Primary antibody (1:1000) was incubated overnight with 5% bovine serum albumin at 4 °C and secondary antibody (horseradish peroxidase conjugated, 1: 20,000) was incubated for 90 minutes with 5% bovine serum albumin at room temperature. Immunoreactivity was detected by enhanced chemiluminescent substrate (Thermo Fisher Scientific, MA).

Masson's trichrome staining

Mid-ventricular heart tissues were cut and stained according to the manufacturer's protocol (Sigma-Aldrich). Fractional myocardial fibrosis (blue-gray pixels divided by total pixels) was measured using ImageJ software.

Statistical analysis

Continuous variables are shown as mean ± standard deviation and categorical variables are presented as percentages. Normal distribution was assessed using Kolmogorov-Smirnov test and homogeneity of variance was tested by Levene's test. Student's t-test (paired or unpaired as appropriate) was used for the comparison of variables with normal distribution, while Wilcoxon rank sum test was used for the comparisons of non-normally distributed variables. Analysis of repeated measures was performed with mixed-model regression to adjust for any possible missing data points with post-hoc testing across groups adjusted for multiple testing (Tukey). Fisher's exact test was used to compare categorical variables (arrhythmia induction rates). Multiple t-tests of RT Q-PCR data across groups was performed using step-down bootstrap sampling to control the familywise error rate at 0.05. Two-tailed p value was used to assess statistical significance (* denotes p value < 0.05 and ** denotes p value < 0.001). SAS V9.4 software was used for analysis.

RESULTS

Development of HFpEF in HS fed rats

Figure 1B-E shows echocardiographic data at 7, 14 and 18 weeks of age. Ejection fraction (EF) was equivalent at baseline (7 weeks) in NS and HS rats, nor did it differ in follow up in the various groups (Fig. 1B). Figure 1C shows representative E and A wave changes from pulse wave Doppler mode and E' and A' wave changes in tissue Doppler mode at 7, 14 and 18 weeks of age. Pooled data reveal that baseline E/A ratios did not differ between NS and HS rats; however, by 14 weeks, E/A ratio in HS rats decreased (1.25±0.24 vs. 1.56±0.13 in NS, $p < 0.001$) verifying the development of diastolic dysfunction (Fig. 1D). At 18 weeks, E/A ratio in HS rats approached values in NS rats (1.46±0.17 vs. 1.60±0.08, p=0.27) consistent with pseudo-normalization of E/A ratio as seen in the progression of diastolic dysfunction[22, 41] (Fig. 1D). While no differences in E/E' ratio were seen at 7 weeks, E/E' increased in HS rats at 14 and 18 weeks (p=0.011 at 14 weeks and $p < 0.001$ at 18 weeks; Fig. 1E). Unlike E/A ratio, E/E' rises monotonically as diastolic dysfunction progresses,[42] and is thus helpful in differentiating salutary from pseudo-normal changes in E/A ratio (Fig.

1C). To define the normal range for diastolic function, we plotted 95% distribution values (2.5% to 97.5%) of E/A ratio and E/E' ratio of 13 normal-salt rats at 14 weeks of age (Fig. 1F-G), which yielded normal E/A of 1.30–1.80 and 9.86–17.19 for E/E'. Diastolic dysfunction was defined as either E/A ratio < 1.30 or E/E' > 17.19 (Fig. 1F-G). Of 38 HS rats, 31 were verified to have diastolic dysfunction. Such rats showed signs of HF such as weakness, decreased activity, labored breathing, or body edema starting from 14 weeks of age, and so were classified as having not only diastolic dysfunction but also HFpEF.

Increased susceptibility to VA in HFpEF rats

PES was performed *in vivo* in control (n=13) and HFpEF (n=31) rats at 14–16 weeks. In control animals, VA were induced only in 3 of 13 (23.1%) rats after PES (Supplemental Video 1, no induction of arrhythmia in a control rat). In contrast, VA were induced in 27 of 31 (87.1%) HFpEF rats. The VA were monomorphic in 7 of 27 inducible HFpEF rats, but most (20 of 27 [74%]) showed polymorphic ventricular tachycardia (VT) or ventricular fibrillation (VF) (Fig. 2A-B) (Supplemental Video 2, induction of polymorphic VT in a HFpEF rat). The propensity to develop VT/VF after PES was not only higher in HFpEF animals ($p < 0.001$), but also they were easier to induce by PES compared to controls (Fig. 2C). Interestingly, the duration of induced VA was longer in HFpEF rats compared to controls (Fig. 2D). We defined AI as a single parameter that takes into account the duration of the arrhythmias and the aggressiveness of the PES protocol; this number was markedly increased in HFpEF rats (30.1±20.0 vs. 3.9±8.1 in controls, $p < 0.001$; Fig. 2E).

ECG analyses in control and HFpEF rats

By surface ECG, no conduction delays were evident in HFpEF animals at 14 or 18 weeks, relative to controls (PR interval data in Fig. 3A; QRS interval in Fig. 3B). However, repolarization (as manifested by QT and QTc interval) was prolonged in HFpEF rats, as evident from the representative electrocardiograms in Fig. 3 C-E. Pooled data confirm QT increases at 14 weeks (111.1±18.0 vs. 81.8±5.9 ms in controls, $p < 0.001$) and even more so with progression of the disease at 18 weeks (126.5±10.1 vs. 88.5±8.1 ms in controls, $p < 0.001$) (Fig. 3D). QTc showed the same trend at 14 weeks (251.9±27 vs. 192.7±11 ms in controls, $p < 0.001$) and at 18 weeks (281.3±13 vs. 203.3±21 ms in controls, $p < 0.001$) (Fig. 3E). However, heart rate (reported here by RR interval) was not different among groups (Fig. 3F). The observed QTc prolongation prompted us to question whether repolarization reserve might be decreased in HFpEF. We tested this prediction by infusing cesium chloride (Cs), a non-selective potassium channel blocker, intravenously at a final concentration of 1 mM (10 ml), and magnesium sulfate (Mg, 100 mg in 1 ml) to counter the effects. Figure 4A-B shows typical results; Cs increased the tendency to VA inducibility, while Mg suppressed VA. Overall, Cs prolonged QTc in HFpEF rats ($p=0.011$), and increased AI ($p=0.047$; Fig. 4C), while Mg abbreviated QTc ($p=0.039$) and markedly decreased AI ($p=0.007$) (Fig. 4D). Control rats exhibited a trend towards QTc prolongation after Cs administration (192.0±7 to 213.6±15 ms, $p=0.069$), but VA were not induced (Fig. 4E).

Optical mapping in Langendorff-perfused hearts

During *ex vivo* perfusion of isolated hearts, optical mapping revealed action potentials evoked by pacing at 100, 200 and 300 ms cycle length. Figure 5A-B shows representative

action potential recordings in control and HFpEF rat hearts at 300 ms cycle length. Restitution curve shows APD90 prolongation in HFpEF rats (142.8±12.4 vs. 97.3±4.5 ms in controls, p=0.002) at 300 ms cycle length and at 200 ms cycle length (115.0±8.3 vs. 83.0±5.6 ms in controls, p=0.003) (Fig. 5C). In HFpEF rats, APD was widely dispersed and heterogeneous compared to controls (standard deviation of APD90 11.1±2.0 VS 4.0±1.2, p=0.001) (Fig. 5D-E). Additionally, *ex vivo* PES demonstrated inducible VT/VF in HFpEF hearts (Fig. 5F). Analysis of the activation patterns showed both clockwise and counter-clockwise conduction in the left ventricle, suggesting multiple re-entry circuits as the arrhythmia mechanism (Fig. 5G) (Supplemental Video 3, multiple re-entry circuits). Importantly the site of block (first beat of VT in Fig. 5G) was found to be located at the region where the APD dispersion was high (APD map in Fig. 5F) and this created the first re-entry circuit for the arrhythmia which can implicate the importance of APD dispersion as the functional re-entry mechanism.

Single-cell electrophysiology

Action potentials were longer in HFpEF cardiomyocytes than in controls, as is evident from the representative records superimposed in Fig. 6A. Such differences were consistent: Fig. 6B shows that APD90 was prolonged in HFpEF cardiomyocytes (175.0±21.1 vs. 90.5±12.5 ms in controls, p=0.001). The action potential amplitude was not statistically different in the two groups (89.4±18.2 vs. 94.9±18.0 mV, p=0.52) (Supplemental Fig. 1A). Single-cell recordings also give us the opportunity to measure capacitance as an index of cell surface area. Consistent with the hypertrophy seen *in vivo* by echocardiography in HFpEF rats, membrane capacitance was increased in HFpEF cardiomyocytes (265.8±15.5 vs. 199.7±10.2 pF in controls, $p < 0.001$) supporting the idea that the wall is thick in HS rats because cardiomyocytes enlarge (Fig. 6C), consistent with previous observations.[21] Given the observed delay of repolarization, we quantified the density of transient outward potassium current (I_{to}), which is the major repolarizing current in rodent hearts.[43] Compared to cardiomyocytes from control animals, I_{to} was decreased in cardiomyocytes from HFpEF rats (4.13±1.78 vs. 8.03±3.75 pA/pF in controls at 60 mV, $p < 0.05$) (Fig. 6D-E). Reductions in I_{to} have been documented in multiple models of HFrEF, but not previously in HFpEF. The rapid component of delayed rectifier potassium current (I_{Kr}) was also decreased in HFpEF rats (0.92±0.52 vs. 2.46±1.28 pA/pF in controls at 60 mV, $p < 0.05$) (Fig. 6F-G). However, due to the relatively low density of the current, the contribution of I_{Kr} to the repolarization duration will be smaller than that of I_{to}. The inward rectifier potassium current (I_{K1}) was also revealed to be down-regulated in HFpEF rats (−7.58±4.90 vs. −16.81±5.50 pA/pF in controls at −120 mV, $p < 0.05$) (Fig. 6H-I). However, the changes are smaller in the physiologic range (−70 to +10 mV). In contrast to the prevailing down-regulation of K currents, L-type Ca current (I_{CaL}) was modestly increased in HFpEF rats (-6.60±1.27 vs. −5.18±0.75 pA/pF in controls at 0 mV, $p < 0.05$) (Supplemental Figure 1B-C). The changes all favor prolonged repolarization.

Contribution of I_{to} to increased arrhythmogenicity

NS5806, a known I_{to} activator, was able to shorten QTc interval in HFpEF rats (254.9±10.4 ms to 224.1±16.8 ms, $p < 0.05$); however, this drug did not significantly alter arrhythmogenicity (AI 34.5±9.9 to 30.0±5.7, p=0.22) (Supplemental Figure 1D-E). This

finding indicates that factors other than mean I_{to} density are major contributors to the risk of ventricular arrhythmia in HFpEF rats.

Quantitative polymerase chain reaction and western blot

Concordant with the changes seen in single-cell electrophysiology, mRNA level of I_{to}–related potassium channel gene was decreased in HFpEF rat hearts (*Kcnd2*, p=0.26; *Kcnd3*, p=0.046) (Fig. 7A). In contrast, transcript levels of several non-I_{to} ion channel genes (*Scn5a* [I_{Na}], *Cacna1c* and *Cacna1d* [I_{Ca}], *Kcna5* [I_{Kur}], *Kcnh2* [I_{Kr}], *Kcnq1* [I_{Ks}] and *Kcnj2* [I_{K1}]) were not significantly different from controls. To verify changes of *Kcnd2* and *Kcnd3* genes at the protein level, we performed western blots of these gene products (Kv4.2 and Kv4.3) (Fig. 7B-C). Kv4.2 expression was similar in the two groups (Fig. 7D), but, Kv4.3 expression was decreased in HFpEF (0.32±0.03 vs. 0.65±0.07 in controls, p=0.01) (Fig. 7E). Kv4.3 is the dominant isoform contributing to I_{to} in rodents.[43] These results are consistent with the notion that down-regulation of I_{to} is attributable to decreased *Kcnd3* transcription hence decreased Kv4.3 expression in HFpEF cardiomyocytes. Western blots for Kv1.4 (another I_{to}-related protein) were not significantly different between control and HFpEF rats (Supplemental Fig. 2A-B). Kv11.1 (protein for I_{Kr}) and Kir2.1 (protein for I_{K1}) were not changed between the two groups (Supplemental Fig. 2C-F).

Fibrosis

The extent of fibrosis, measured with Masson's trichrome staining, increased in HFpEF hearts compared to control hearts (9.96±1.29 % vs 2.21±0.75 % in controls, $p < 0.001$) (Fig. 7F-G). Increased fibrosis favors anatomical re-entry and thus contributes to arrhythmogenesis.

DISCUSSION

Here we have investigated the mechanisms of arrhythmogenesis in HFpEF. Using DSS rats, we found that phenotypically-verified HFpEF increases the inducibility of VA by PES due to delayed repolarization and multiple re-entry circuits (Fig. 8). In addition to being more frequently inducible, fewer extra stimuli were needed to elicit VA, and such VA lasted longer in HFpEF rats. While the increase in VA inducibility may be exacerbated by the increase in myocardial fibrosis in this model,[21] we also have discovered that HFpEF is accompanied by abnormal repolarization: surface ECGs showed QTc prolongation, action potentials were prolonged in single-cell recordings, and *ex vivo* optical mapping revealed increased APD90 as well as VA with a torsades-like migratory re-entrant pattern. Underlying the increased arrhythmic risk we found prolonged repolarization, down-regulation of I_{to}, and reductions in I_{to}–relevant transcript (*Kcnd3*) and protein (Kv4.3) levels. While some HFpEF rats developed monomorphic VT, 74% exhibited polymorphic VT. Such rats consistently showed multiple re-entry circuits by *ex vivo* optical mapping. This rat model of HFpEF mimics human HFpEF in terms of diastolic dysfunction, QTc prolongation, high sudden death rate, increased fibrosis and the presence of hypertension as a comorbidity (Table 1). In a number of other respects, however, the Dahl salt-sensitive rat differs from human HFpEF: non-hypertensive co-morbidities are absent in the rat, and resting heart rate is not elevated in the

disease state. Thus, the data from the HFpEF rat model should be considered hypothesis-generating with respect to arrhythmogenesis in the human condition.

Despite the increasing prevalence of the disease, there has been a lamentable paucity of basic research on HFpEF. For the past decade, the Dahl salt-sensitive rat has been validated as a reasonable model of HFpEF by different groups.[21–23, 44, 45] The animals develop diastolic dysfunction after 6–7 weeks of high-salt diet along with abnormal relaxation and elevated left ventricular end-diastolic pressure.[21–23] Concurrently, rats develop HF symptoms including decreased activity, cachexia, labored breathing, and body edema starting from 14 weeks old.[21] Nevertheless, there is some variability in the responses of DSS rats to high-salt, making it important to confirm the presence of HFpEF echocardiographically and clinically before classifying an animal as suffering from the condition.

Investigating the mechanisms of SCD in animal models is often challenging due to the relatively low incidence of VA, and the sudden nature of the disease. Arrhythmias are believed to be the cause of SCD in most cases of HF.[9, 10, 13] Since it is difficult to document the spontaneous development of VA in rats, we applied PES to induce arrhythmias in our experimental model of HFpEF. VA induction by PES has been clinically validated to predict the risk of SCD in patients.[29] In our model, HFpEF rats were not only more easily inducible, but also had more prolonged VA compared to controls.

Delayed repolarization due to down-regulation of I_{to} has been a recurrent theme in HFrEF animal models and humans.[9, 10, 13] Although I_{to} is considered the major repolarizing current in rat cardiomyocytes, this current is smaller in humans; nevertheless, down-regulation of I_{to} has been associated with marked prolongation of action potentials in human HFrEF.[15, 16] Our rat model of HFpEF showed decreased I_{to} as well as I_{Kr} density, which can potentiate the prolongation of action potential. Although I_{Kr} is a minor current in rat cardiomyocytes, it plays a crucial role in human cardiac repolarization. Prolongation of the QTc occurs in HFpEF patients, and correlates with the degree of diastolic dysfunction.[46] Furthermore, QTc prolongation is associated with increased mortality in HF patients and SCD in an older population cohort.[47, 48] The “reasons” for delayed repolarization remain unclear. Prolonged APD can theoretically offset systolic failure by prolonging the elevation in activator Ca^{2+} during each cardiac cycle, at least in HFrEF. In contrast, the prolongation of repolarization in HFpEF is maladaptive, truncating the time available for ventricular relaxation. In both HFrEF and HFpEF, repolarization delay may favor opportunistic re-entry and long QT-type arrhythmogenesis. We have shown multiple re-entrant circuits underlying VA. The combination of prolonged repolarization, increased fibrosis and inflammation would logically be expected to favor QT dispersion and opportunistic re-entry in HFpEF.[21] Furthermore, prolonged repolarization induces the instability of the repolarizing action potential, hence can provoke afterdepolarizations which can potentially initiate VA. Therapies targeting these various processes merit further investigation.

Some limitations of the present study should be noted. First, while this HFpEF model has been extensively validated, its relevance to human HFpEF is uncertain, although hypertension is a major comorbidity in human HFpEF. Second, although VA inducibility by

PES is not necessarily a reliable surrogate of spontaneous arrhythmias and SCD, this well-controlled intervention can nevertheless provide mechanistic insights which can be tested in the prospective prevention of SCD. Although I_{to} correlated well with underlying transcript and protein levels, the changes among I_{Kr}, I_{K1} and the relevant mRNA and proteins were not concordant. Further investigation into the underling mechanisms was beyond the scope of this initial report.

Supplementary Material

Refer to Web version on PubMed Central for supplementary material.

Acknowledgments

None

SOURCES OF FUNDING

This research was supported by NIH T32 HL116273, and Department of Defense grant PR150620.

References

1. Kochanek KD, Murphy SL, Xu J, Tejada-Vera B. Deaths: Final Data for 2014. Natl Vital Stat Rep. 2016; 65:1–122.
2. Yancy CW, Jessup M, Bozkurt B, Butler J, Casey DE Jr, Drazner MH, Fonarow GC, Geraci SA, Horwich T, Januzzi JL, Johnson MR, Kasper EK, Levy WC, Masoudi FA, McBride PE, McMurray JJ, Mitchell JE, Peterson PN, Riegel B, Sam F, Stevenson LW, Tang WH, Tsai EJ, Wilkoff BL. Writing Committee M; American College of Cardiology Foundation/American Heart Association Task Force on Practice G. 2013 ACCF/AHA guideline for the management of heart failure: a report of the American College of Cardiology Foundation/American Heart Association Task Force on practice guidelines. Circulation. 2013; 128:e240–327. [PubMed: 23741058]
3. Jessup M, Brozena S. Heart failure. N Engl J Med. 2003; 348:2007–2018. [PubMed: 12748317]
4. Braunwald E. Heart failure. JACC Heart Fail. 2013; 1:1–20. [PubMed: 24621794]
5. Owan TE, Hodge DO, Herges RM, Jacobsen SJ, Roger VL, Redfield MM. Trends in prevalence and outcome of heart failure with preserved ejection fraction. N Engl J Med. 2006; 355:251–259. [PubMed: 16855265]
6. Udelson JE. Heart failure with preserved ejection fraction. Circulation. 2011; 124:e540–543. [PubMed: 22105201]
7. Aurigemma GP, Gaasch WH. Clinical practice. Diastolic heart failure. N Engl J Med. 2004; 351:1097–1105. [PubMed: 15356307]
8. Kass DA, Bronzwaer JG, Paulus WJ. What mechanisms underlie diastolic dysfunction in heart failure? Circ Res. 2004; 94:1533–1542. [PubMed: 15217918]
9. Tomaselli GF, Zipes DP. What causes sudden death in heart failure? Circ Res. 2004; 95:754–763. [PubMed: 15486322]
10. Tomaselli GF, Beuckelmann DJ, Calkins HG, Berger RD, Kessler PD, Lawrence JH, Kass D, Feldman AM, Marban E. Sudden cardiac death in heart failure. The role of abnormal repolarization. Circulation. 1994; 90:2534–2539. [PubMed: 7955213]
11. Cohn JN, Johnson G, Ziesche S, Cobb F, Francis G, Tristani F, Smith R, Dunkman WB, Loeb H, Wong M, Bhat G, Goldman S, Fletcher RD, Doherty J, Huges CV, Carson P, Cintron G, Shabetai R, Haakenson MSC. A comparison of enalapril with hydralazine-isosorbide dinitrate in the treatment of chronic congestive heart failure. N Engl J Med. 1991; 325:303–310. [PubMed: 2057035]
12. Zile MR, Gaasch WH, Anand IS, Haass M, Little WC, Miller AB, Lopez-Sendon J, Teerlink JR, White M, McMurray JJ, Komajda M, McKelvie R, Ptaszynska A, Hetzel SJ, Massie BM, Carson

PE, Investigators IP. Mode of death in patients with heart failure and a preserved ejection fraction: results from the Irbesartan in Heart Failure With Preserved Ejection Fraction Study (I-Preserve) trial. Circulation. 2010; 121:1393–1405. [PubMed: 20231531]

13. Tomaselli GF, Marban E. Electrophysiological remodeling in hypertrophy and heart failure. Cardiovasc Res. 1999; 42:270–283. [PubMed: 10533566]
14. Akar FG, Rosenbaum DS. Transmural electrophysiological heterogeneities underlying arrhythmogenesis in heart failure. Circ Res. 2003; 93:638–645. [PubMed: 12933704]
15. Beuckelmann DJ, Nabauer M, Erdmann E. Alterations of K+ currents in isolated human ventricular myocytes from patients with terminal heart failure. Circ Res. 1993; 73:379–385. [PubMed: 8330380]
16. Kaab S, Dixon J, Duc J, Ashen D, Nabauer M, Beuckelmann DJ, Steinbeck G, McKinnon D, Tomaselli GF. Molecular basis of transient outward potassium current downregulation in human heart failure: a decrease in Kv4.3 mRNA correlates with a reduction in current density. Circulation. 1998; 98:1383–1393. [PubMed: 9760292]
17. Nattel S, Maguy A, Le Bouter S, Yeh YH. Arrhythmogenic ion-channel remodeling in the heart: heart failure, myocardial infarction, and atrial fibrillation. Physiol Rev. 2007; 87:425–456. [PubMed: 17429037]
18. Exner DV, Dries DL, Waclawiw MA, Shelton B, Domanski MJ. Beta-adrenergic blocking agent use and mortality in patients with asymptomatic and symptomatic left ventricular systolic dysfunction: a post hoc analysis of the Studies of Left Ventricular Dysfunction. J Am Coll Cardiol. 1999; 33:916–923. [PubMed: 10091816]
19. Effects of enalapril on mortality in severe congestive heart failure. Results of the Cooperative North Scandinavian Enalapril Survival Study (CONSENSUS). The CONSENSUS Trial Study Group. N Engl J Med. 1987; 316:1429–1435. [PubMed: 2883575]
20. Moss AJ, Zareba W, Hall WJ, Klein H, Wilber DJ, Cannom DS, Daubert JP, Higgins SL, Brown MW, Andrews ML. Multicenter Automatic Defibrillator Implantation Trial III. Prophylactic implantation of a defibrillator in patients with myocardial infarction and reduced ejection fraction. N Engl J Med. 2002; 346:877–883. [PubMed: 11907286]
21. Gallet R, de Couto G, Simsolo E, Valle J, Sun B, Liu W, Tseliou E, Zile MR, Marban E. Cardiosphere-derived cells reverse heart failure with preserved ejection fraction (HFpEF) in rats by decreasing fibrosis and inflammation. JACC Basic Transl Sci. 2016; 1:14–28. [PubMed: 27104217]
22. Doi R, Masuyama T, Yamamoto K, Doi Y, Mano T, Sakata Y, Ono K, Kuzuya T, Hirota S, Koyama T, Miwa T, Hori M. Development of different phenotypes of hypertensive heart failure: systolic versus diastolic failure in Dahl salt-sensitive rats. J Hypertens. 2000; 18:111–120. [PubMed: 10678551]
23. Klotz S, Hay I, Zhang G, Maurer M, Wang J, Burkhoff D. Development of heart failure in chronic hypertensive Dahl rats: focus on heart failure with preserved ejection fraction. Hypertension. 2006; 47:901–911. [PubMed: 16585423]
24. Liu J, Rigel DF. Echocardiographic examination in rats and mice. Methods Mol Biol. 2009; 573:139–155. [PubMed: 19763926]
25. Roguin A. Henry Cuthbert Bazett (1885–1950)--the man behind the QT interval correction formula. Pacing Clin Electrophysiol. 2011; 34:384–388. [PubMed: 21091739]
26. Cingolani E, Ramirez Correa GA, Kizana E, Murata M, Cho HC, Marban E. Gene therapy to inhibit the calcium channel beta subunit: physiological consequences and pathophysiological effects in models of cardiac hypertrophy. Circ Res. 2007; 101:166–175. [PubMed: 17556655]
27. Jiao KL, Li YG, Zhang PP, Chen RH, Yu Y. Effects of valsartan on ventricular arrhythmia induced by programmed electrical stimulation in rats with myocardial infarction. J Cell Mol Med. 2012; 16:1342–1351. [PubMed: 22128836]
28. Pahor M, Bernabei R, Sgadari A, Gambassi G Jr, Lo Giudice P, Pacifici L, Ramacci MT, Lagrasta C, Olivetti G, Carbonin P. Enalapril prevents cardiac fibrosis and arrhythmias in hypertensive rats. Hypertension. 1991; 18:148–157. [PubMed: 1885222]
29. Zaman S, Sivagangabalan G, Narayan A, Thiagalingam A, Ross DL, Kovoor P. Outcomes of early risk stratification and targeted implantable cardioverter-defibrillator implantation after ST-

elevation myocardial infarction treated with primary percutaneous coronary intervention. Circulation. 2009; 120:194–200. [PubMed: 19581496]

30. Cooper MJ, Hunt LJ, Richards DA, Denniss AR, Uther JB, Ross DL. Effect of repetition of extrastimuli on sensitivity and reproducibility of mode of induction of ventricular tachycardia by programmed stimulation. J Am Coll Cardiol. 1988; 11:1260–1267. [PubMed: 3367000]
31. Lang D, Sulkin M, Lou Q, Efimov IR. Optical mapping of action potentials and calcium transients in the mouse heart. J Vis Exp. 2011; 55:3275.
32. Herron TJ, Lee P, Jalife J. Optical imaging of voltage and calcium in cardiac cells & tissues. Circ Res. 2012; 110:609–623. [PubMed: 22343556]
33. Efimov IR, Nikolski VP, Salama G. Optical imaging of the heart. Circ Res. 2004; 95:21–33. [PubMed: 15242982]
34. Laughner JI, Ng FS, Sulkin MS, Arthur RM, Efimov IR. Processing and analysis of cardiac optical mapping data obtained with potentiometric dyes. Am J Physiol Heart Circ Physiol. 2012; 303:H753–765. [PubMed: 22821993]
35. Asano Y, Davidenko JM, Baxter WT, Gray RA, Jalife J. Optical mapping of drug-induced polymorphic arrhythmias and torsade de pointes in the isolated rabbit heart. J Am Coll Cardiol. 1997; 29:831–842. [PubMed: 9091531]
36. Morita N, Lee JH, Xie Y, Sovari A, Qu Z, Weiss JN, Karagueuzian HS. Suppression of reentrant and multifocal ventricular fibrillation by the late sodium current blocker ranolazine. J Am Coll Cardiol. 2011; 57:366–375. [PubMed: 21232675]
37. Weber dos Santos R, Nygren A, Otaviano Campos F, Koch H, Giles WR. Experimental and theoretical ventricular electrograms and their relation to electrophysiological gradients in the adult rat heart. Am J Physiol Heart Circ Physiol. 2009; 297:H1521–1534. [PubMed: 19700625]
38. Fukumoto GH, Lamp ST, Motter C, Bridge JH, Garfinkel A, Goldhaber JI. Metabolic inhibition alters subcellular calcium release patterns in rat ventricular myocytes: implications for defective excitation-contraction coupling during cardiac ischemia and failure. Circ Res. 2005; 96:551–557. [PubMed: 15718501]
39. Fiset C, Clark RB, Shimoni Y, Giles WR. Shal-type channels contribute to the Ca2+-independent transient outward K+ current in rat ventricle. J Physiol. 1997; 500(Pt 1):51–64. [PubMed: 9097932]
40. Wickenden AD, Jegla TJ, Kaprielian R, Backx PH. Regional contributions of Kv1.4, Kv4.2, and Kv4.3 to transient outward K+ current in rat ventricle. Am J Physiol. 1999; 276:H1599–607. [PubMed: 10330244]
41. Nagueh SF, Smiseth OA, Appleton CP, Byrd BF 3rd, Dokainish H, Edvardsen T, Flachskampf FA, Gillebert TC, Klein AL, Lancellotti P, Marino P, Oh JK, Popescu BA, Waggoner AD. Recommendations for the Evaluation of Left Ventricular Diastolic Function by Echocardiography: An Update from the American Society of Echocardiography and the European Association of Cardiovascular Imaging. J Am Soc Echocardiogr. 2016; 29:277–314. [PubMed: 27037982]
42. Little WC, Oh JK. Echocardiographic evaluation of diastolic function can be used to guide clinical care. Circulation. 2009; 120:802–809. [PubMed: 19720946]
43. Hoppe UC, Marban E, Johns DC. Molecular dissection of cardiac repolarization by in vivo Kv4.3 gene transfer. J Clin Invest. 2000; 105:1077–1084. [PubMed: 10772652]
44. Bowen TS, Rolim NP, Fischer T, Baekkerud FH, Medeiros A, Werner S, Bronstad E, Rognmo O, Mangner N, Linke A, Schuler G, Silva GJ, Wisloff U, Adams V. Optimex Study G. Heart failure with preserved ejection fraction induces molecular, mitochondrial, histological, and functional alterations in rat respiratory and limb skeletal muscle. Eur J Heart Fail. 2015; 17:263–272. [PubMed: 25655080]
45. Adams V, Alves M, Fischer T, Rolim N, Werner S, Schutt N, Bowen TS, Linke A, Schuler G, Wisloff U. High-intensity interval training attenuates endothelial dysfunction in a Dahl salt-sensitive rat model of heart failure with preserved ejection fraction. J Appl Physiol (1985). 2015; 119:745–752. [PubMed: 26229002]
46. Wilcox JE, Rosenberg J, Vallakati A, Gheorghiade M, Shah SJ. Usefulness of electrocardiographic QT interval to predict left ventricular diastolic dysfunction. Am J Cardiol. 2011; 108:1760–1766. [PubMed: 21907948]

47. Vrtovec B, Delgado R, Zewail A, Thomas CD, Richartz BM, Radovancevic B. Prolonged QTc interval and high B-type natriuretic peptide levels together predict mortality in patients with advanced heart failure. Circulation. 2003; 107:1764–1769. [PubMed: 12665499]

48. Straus SM, Kors JA, De Bruin ML, van der Hooft CS, Hofman A, Heeringa J, Deckers JW, Kingma JH, Sturkenboom MC, Stricker BH, Witteman JC. Prolonged QTc interval and risk of sudden cardiac death in a population of older adults. J Am Coll Cardiol. 2006; 47:362–367. [PubMed: 16412861]

CLINICAL PERSPECTIVE

What is new?

- Delayed repolarization underlies increased arrhythmogenesis in rats with HFpEF.
- Multiple re-entry circuits due to action potential prolongation and dispersion contribute to the increased arrhythmogenesis.
- Down-regulation of potassium currents (I_{to}, I_{Kr} and I_{K1}) is responsible for the action potential prolongation.

What are the clinical implications?

- Abnormal repolarization, as reflected by QTc interval prolongation, may play a mechanistic role in HFpEF-associated sudden death.
- Action potential prolongation and increased fibrosis are logical therapeutic targets to decrease arrhythmic risk in HFpEF patients.

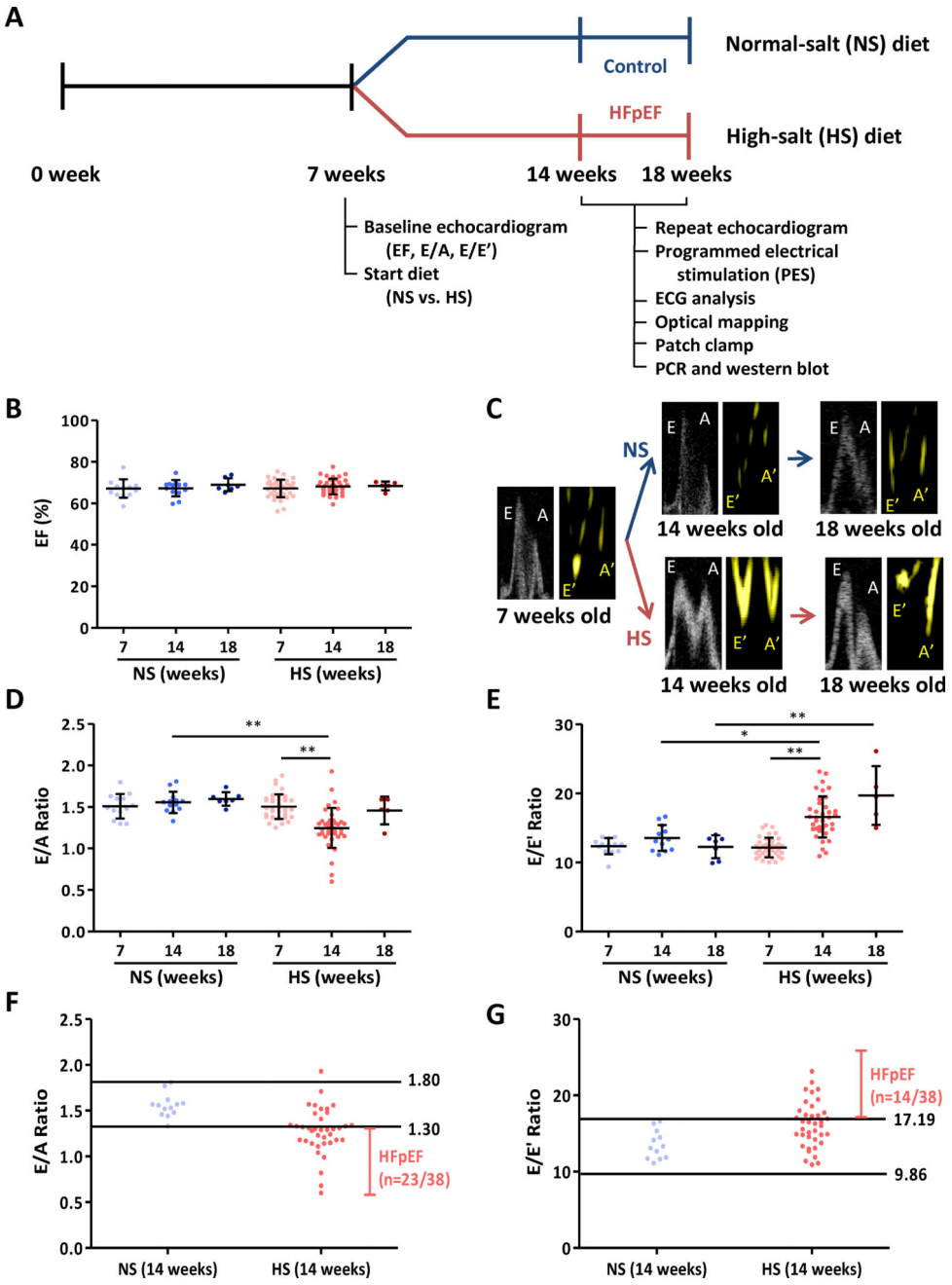

Figure 1. Timeline of experiments and echocardiographic parameters of systolic and diastolic function

A. Dahl salt-sensitive (DSS) rats were fed high-salt (HS, n=38) and normal-salt (NS, n=13) diet at 7 weeks of age after baseline echocardiography for ejection fraction (EF) as a systolic parameter and E/A and E/E' ratios as diastolic markers. Repeat echocardiogram was performed at 14 weeks of age. For control and HFpEF rats 14–18 weeks of age, we performed programmed electrical stimulation (PES), ECG analysis, optical mapping, patch clamp, RT-PCR and western blot. **B**. EF was equivalent at baseline (7 weeks) in NS and HS rats (n=13 and 38 respectively), nor did it differ in follow up in the various groups (n=13 and

38 respectively at 14 weeks, n=7 and 5 respectively at 18 weeks). **C**. Representative pulse wave Doppler showing E (early filling) and A (atrial filling) wave changes and tissue Doppler describing E' and A' wave changes in NS and HS rats at 14 and 18 weeks of age. **D**. Baseline E/A ratios did not differ between NS and HS rats; however, by 14 weeks E/A ratio in HS rats decreased. At 18 weeks, E/A ratio in HS rats pseudo-normalized. **E**. E/E' ratio increased in HS fed rats at 14 weeks and continued to increase at 18 weeks. **F**. Normal value of E/A ratio was obtained from NS rats at 14 weeks old (1.30–1.80). 23 of 38 HS fed rats showed E/A ratio < 1.30, i.e. diastolic dysfunction. **G**. Normal value of E/E' ratio was set (9.86–17.19) from 14-week-old NS rats. E/E' ratio > 17.19 was shown in 14/38 HS fed rats and taken as evidence of diastolic dysfunction. NS fed rats n=13 at 7 weeks, n=13 at 14 weeks and n=7 at 18 weeks. HS fed rats n=38 at 7 weeks, n=38 at 14 weeks and n=5 at 18 weeks. Error line indicates mean and standard deviation. * denotes $p < 0.05$ and ** denotes $p < 0.001$. Mixed model regression with post-hoc testing (Tukey adjustment) was used for 1B, D and E.

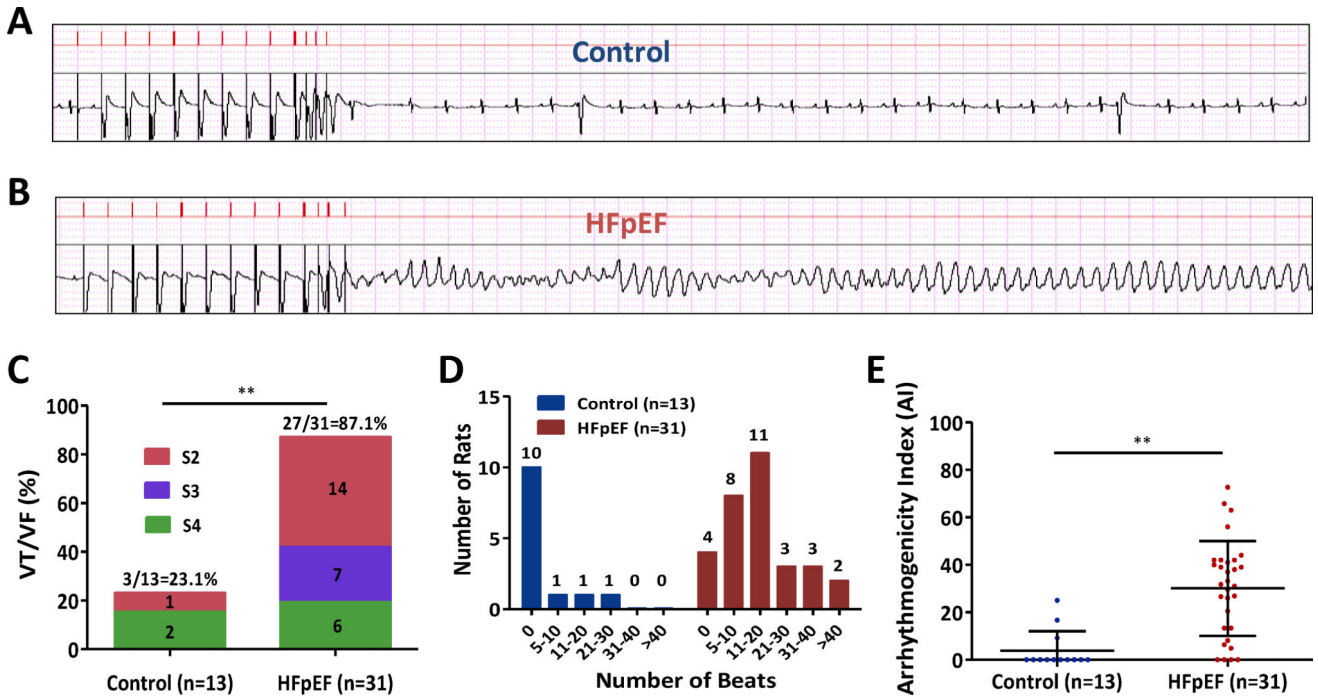

Figure 2. Programmed electrical stimulation (PES) in control and HFpEF rats

A. Representative surface electrograms (upper panel: stimuli, lower panel: ECG) show no inducible arrhythmia in a control rat with S1, S2, S3 and S4 stimuli. **B**. Polymorphic ventricular tachycardia in a HFpEF rat induced by S1, S2, S3 and S4 stimuli. **C**. PES in 13 control and 31 HFpEF rats showed increased susceptibility to VA in HFpEF rats. **D**. HFpEF rats exhibited more prolonged VA compared to control rats. **E**. Arrhythmogenicity index (AI) was increased in HFpEF rats compared to control rats. Control rats n=13 and HFpEF rats n=31. Pooled data lines show mean and standard deviation. ** denotes $p < 0.001$. Fisher's exact test was used in 2C and Wilcoxon rank sum test was used in 2E.

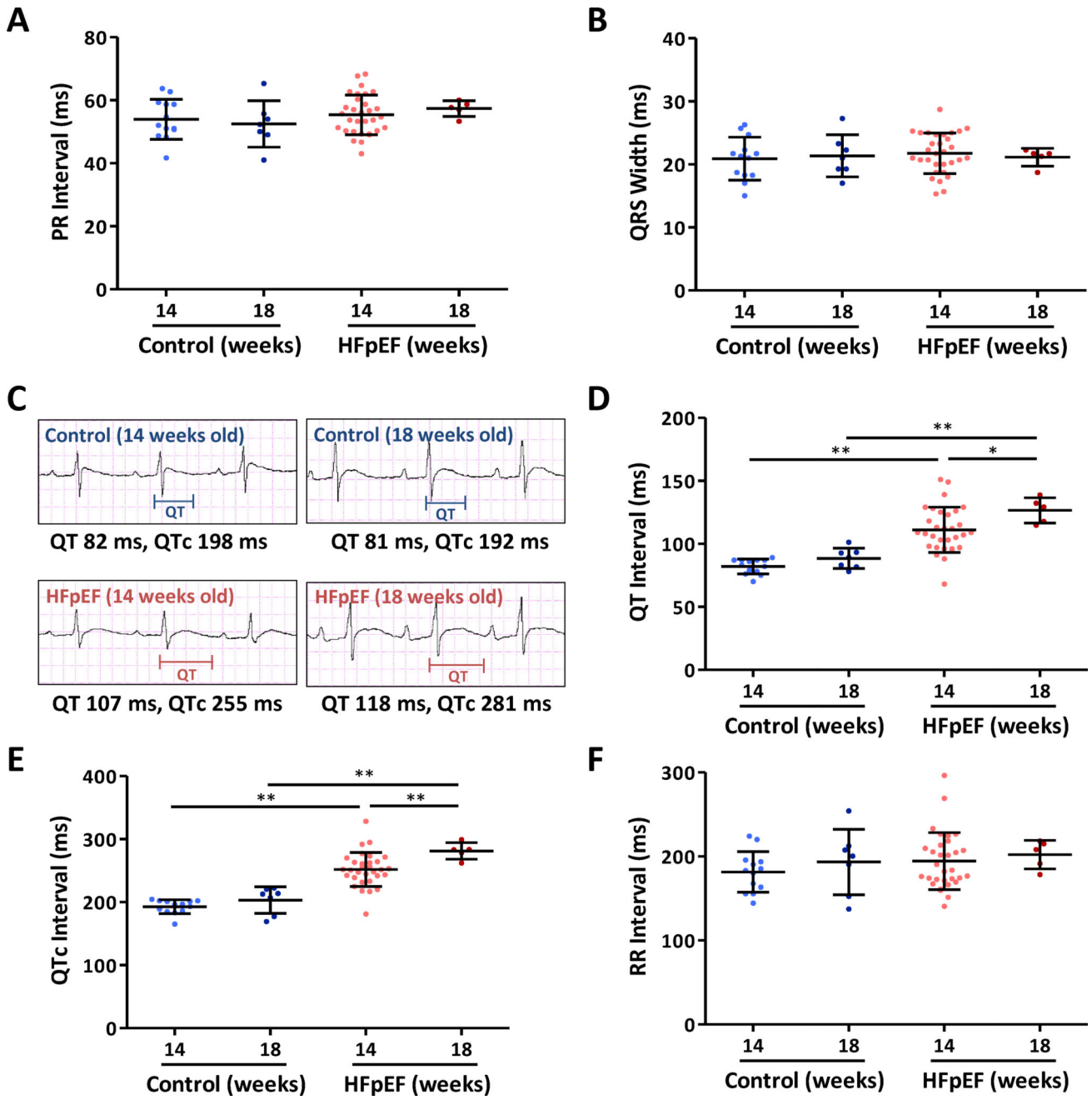

Figure 3. ECG analyses in control and HFpEF rats

PR interval (**A**) and QRS width (**B**) in the two groups at 14 and 18 weeks show no differences between control and HFpEF rats. **C**. Representative ECGs showing QTc prolongation in HFpEF rat compared to control rat at 14 weeks. QTc prolongation in HFpEF rats is more pronounced at 18 weeks of age. **D**. QT interval was prolonged at 14 weeks of age with progression at 18 weeks of age. **E**. QTc was prolonged in HFpEF rats at 14 weeks compared to control rats and the prolongation is more pronounced at 18 weeks old. **F**. RR interval did not differ between the two groups. Control rats n=13 at 14 weeks and n=7 at 18 weeks. HFpEF rats n=31 at 14 weeks and n=5 at 18 weeks. Error line indicates mean and

standard deviation. * denotes $p < 0.05$ and ** denotes $p < 0.001$. Mixed model regression with post-hoc testing (Tukey adjustment) was used for 3A-B and 3D-F.

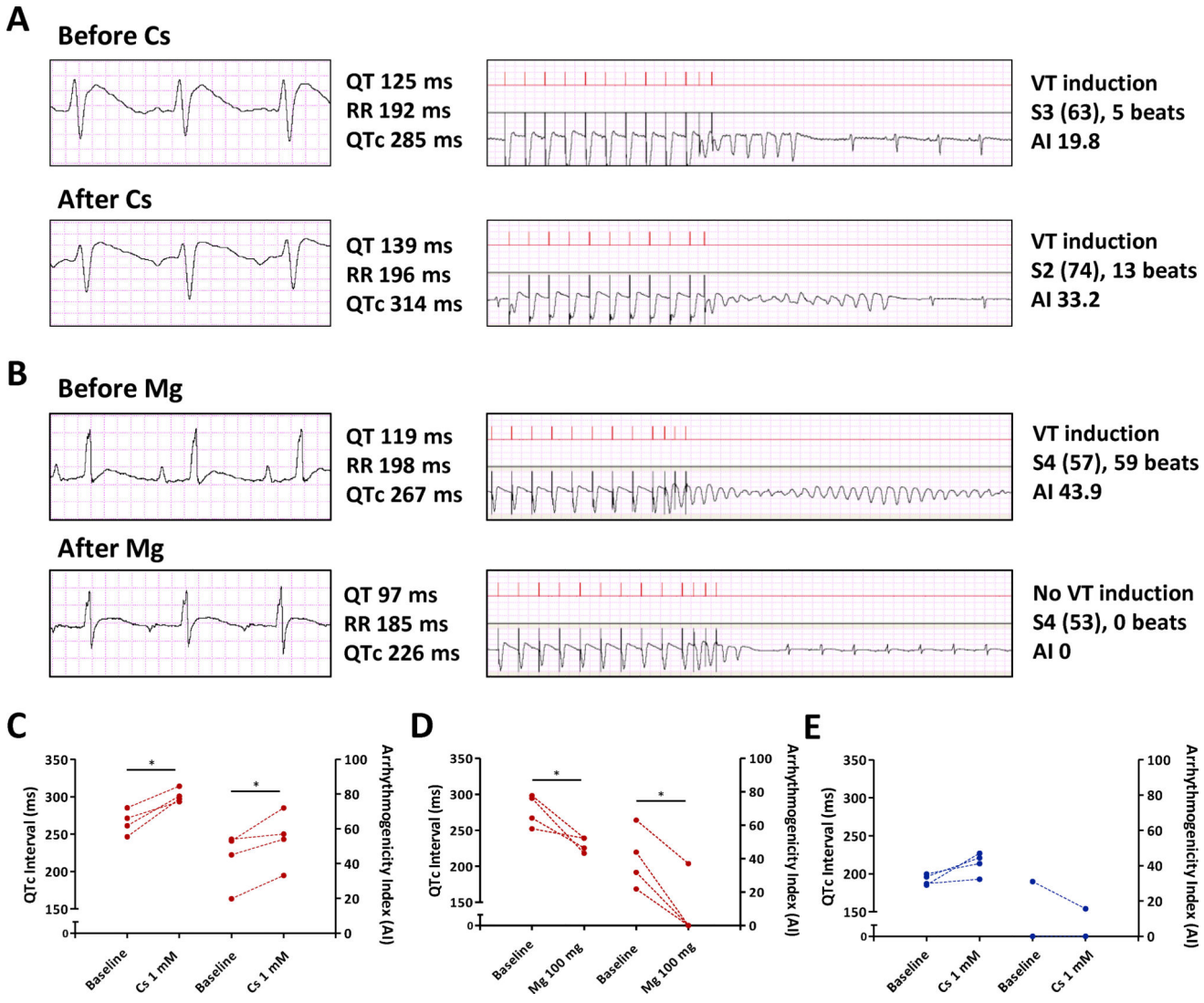

Figure 4. Reduced repolarization reserve in HFpEF rats

A. 10 ml of 1 mM cesium chloride delivered through tail vein in a HFpEF rat prolonged QTc from 285 ms to 314 ms and worsened arrhythmia (AI from 19.8 to 33.2). **B**. 100 mg of magnesium sulfate delivered intravenously in a HFpEF rat decreased QTc interval from 267 ms to 226 ms and abolished the arrhythmia (AI 43.9 to 0). **C**. Cesium chloride prolonged QTc in HFpEF rats (left Y axis) and worsened VA (AI in right Y axis). HFpEF rats n=4. **D**. Magnesium sulfate shortened QTc interval in HFpEF rats (left Y axis) and decreased AI (right Y axis). HFpEF rats n=4. **E**. Cesium chloride in control rats prolonged QTc interval (left Y axis) but failed to induce VA (AI in right Y axis). Control rats n=4. * denotes $p < 0.05$. Paired t-test was used for 4C-E.

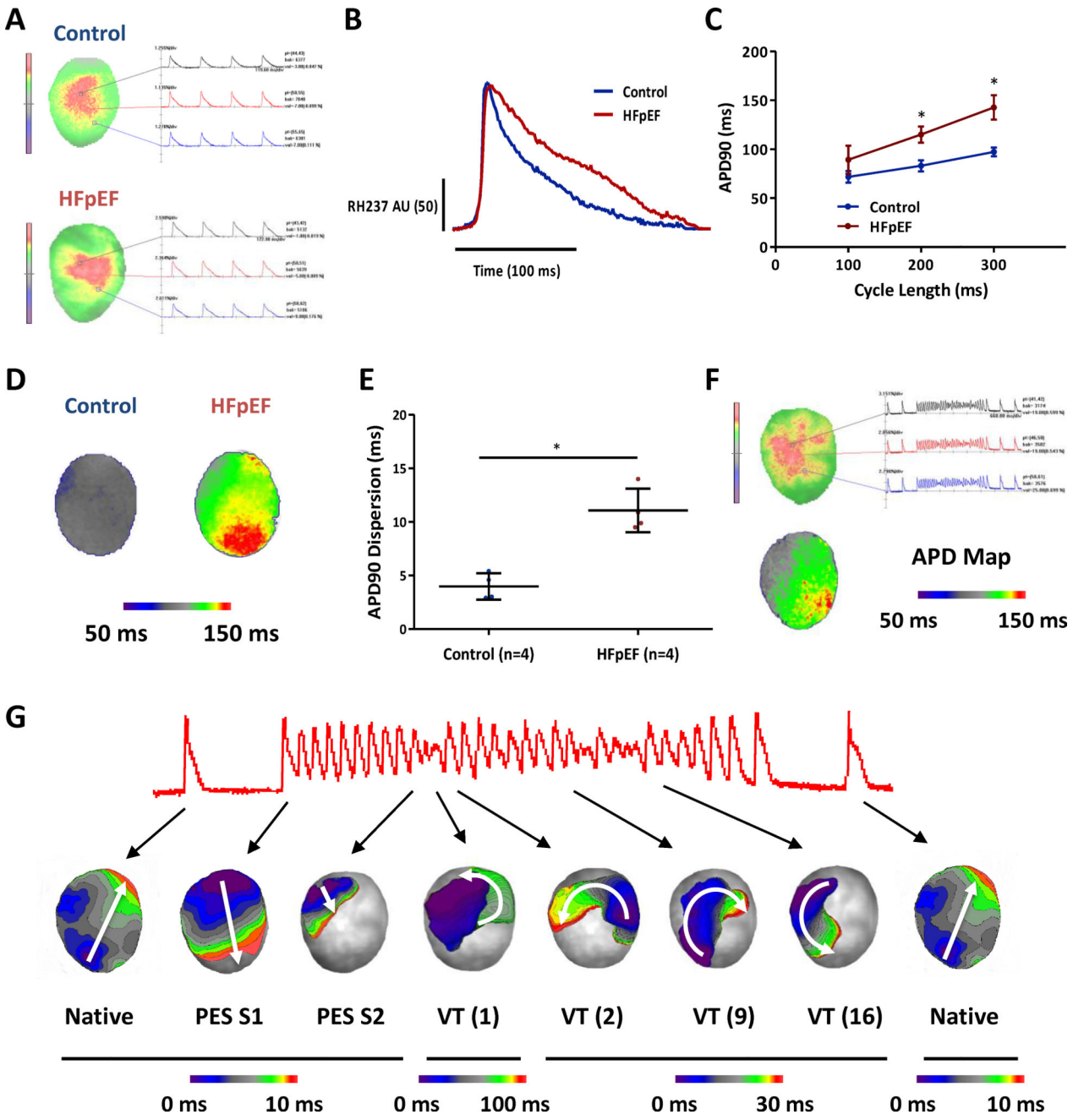

Figure 5. Optical mapping shows prolonged action potentials and polymorphic VT in HFpEF hearts

A. Optical mapping of control and HFpEF hearts *ex vivo* showed action potential changes. **B**. Action potential prolongation in HFpEF is evident in representative recordings. **C**. Action potential duration 90% (APD90) is prolonged in HFpEF hearts compared to control hearts. Control rats n=4 and HFpEF rats n=4. **D**. Representative APD map of control and HFpEF hearts. **E**. APD dispersion was increased in HFpEF rats compared to controls. **F**. PES in a HFpEF rat elicited polymorphic VT. APD map of the rat heart showed heterogenous and dispersed APD **G**. Activation map analyses of the polymorphic VT showed multiple re-entry

circuits. First 10 beats are caused by 10 S1 stimuli and next beat by single S2. There were approximately 22 VT beats and with variable clockwise or counter-clockwise rotation indicating multiple re-entry circuits. Of note, the site of block was found to be located at the region where the APD dispersion was high and this created the first re-entry circuit for the arrhythmia. Error line indicates mean and standard deviation. * denotes $p < 0.05$. AU: Arbitrary Unit. Mixed model regression with post-hoc testing (Tukey adjustment) was used for 5C and unpaired t-test was used for 5E.

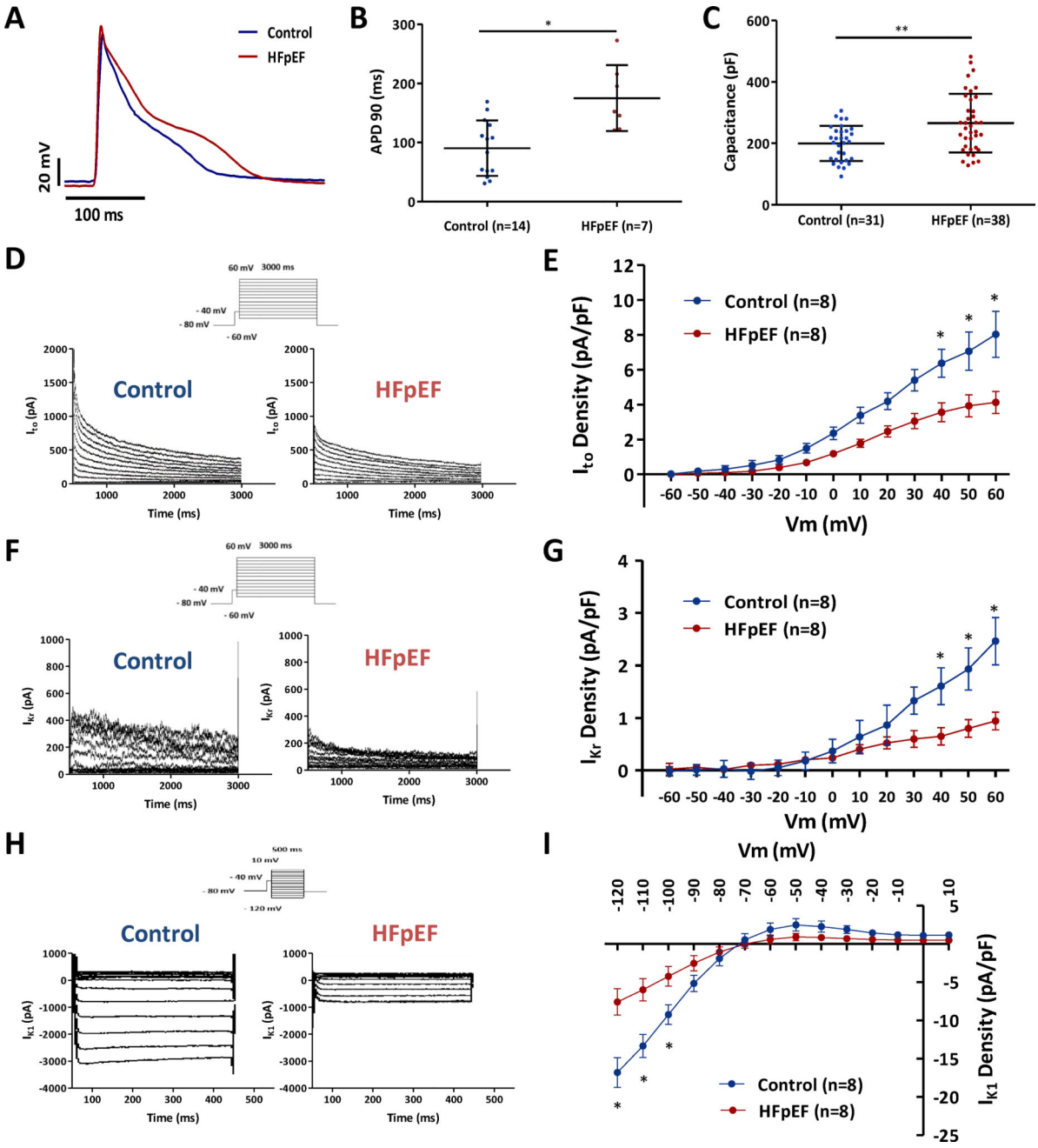

Figure 6. Prolonged action potential duration in HFpEF cardiomyocytes and down-regulation of potassium currents

A. Representative action potentials in control and HFpEF cardiomyocytes. **B**. APD90 was prolonged in HFpEF cardiomyocytes compared to controls (n=14 cells from 4 control rats, and n=7 cells from 4 HFpEF rats). **C**. Cell capacitance was increased in HFpEF compared to control cardiomyocytes (n=31 cardiomyocytes from control rats, and n=38 cardiomyocytes from HFpEF rats). **D, F, H**. Representative I_{to}, I_{Kr} and I_{K1} recordings in control and HFpEF rats. **E, G, I**. Down-regulation of I_{to}, I_{Kr} and I_{K1} density in HFpEF rats compared to control rats (n=8 cardiomyocytes from n=4 rats each group). Error line indicates mean and standard

deviation (6B-C) and standard error of mean (6E, G, I). * denotes $p < 0.05$ and ** denotes $p < 0.001$. Unpaired t-test was used for 6B, Wilcoxon rank sum test was used for 6C, and mixed model regression with post-hoc testing (Tukey adjustment) was used for 6E, G, I.

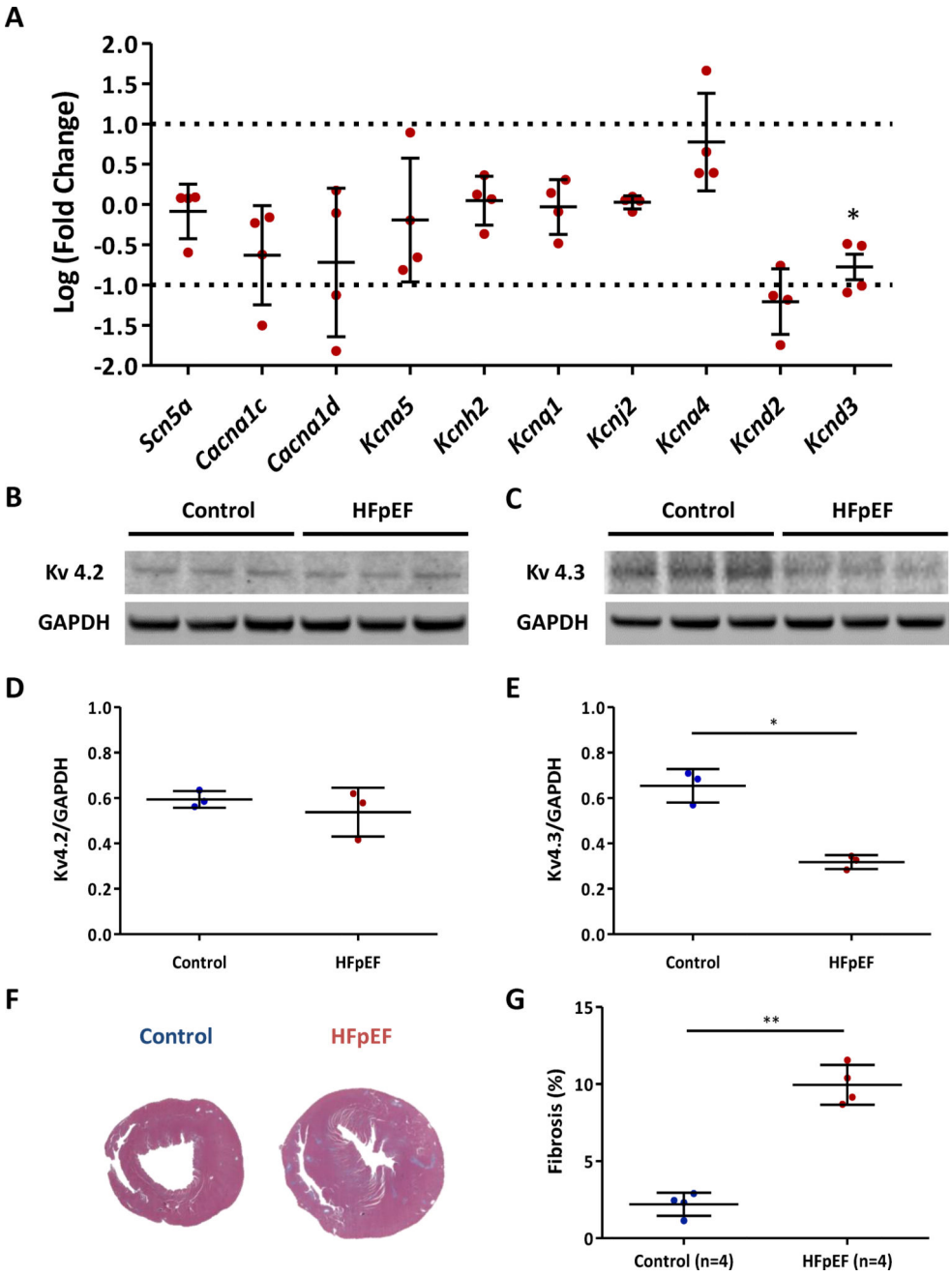

Figure 7. Transcript and protein levels of ion channel genes and fibrosis in control and HFpEF rats

A. Quantitative reverse transcriptase PCR showed decreased expression of *Kcnd2* and *Kcnd3* mRNAs in HFpEF hearts compared to control hearts. Y axis indicates log (fold change). HFpEF rats n=4. **B**. Western blot of Kv4.2 showed no expression differences in the two groups. **C**. Kv4.3 expression was decreased in HFpEF rats compared to control rats. **D**. Kv4.2/GAPDH ratio did not differ between the two groups. n=3 rats each group. **E**. Kv4.3/GAPDH ratio was markedly decreased in HFpEF rats compared to control rats. n=3 rats each group. **F**. Representative Masson's trichrome-stained sections of control and HFpEF

hearts. **G**. Increased fibrosis in HFpEF hearts compared to controls. Error line indicates mean and standard deviation. * denotes $p < 0.05$ and ** denotes $p < 0.001$. Multiple t-tests were performed using step-down bootstrap sampling to control the familywise error rate at 0.05 for 7A, D and E, and unpaired t-test was used for 7G.

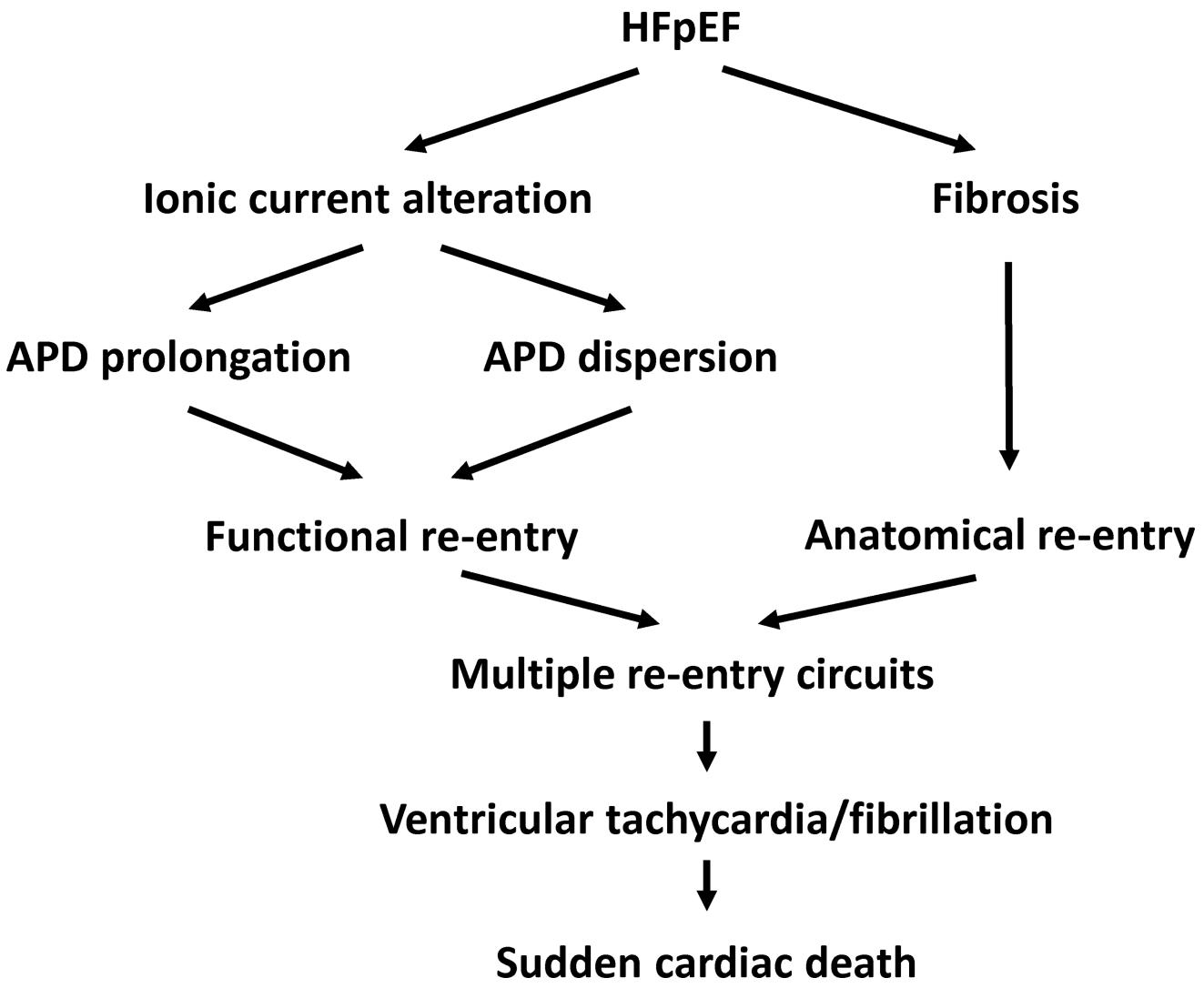

Figure 8. Schematic representation of our working hypothesis

Increased susceptibility to VA in HFpEF is proposed to be due to action potential prolongation/dispersion and fibrosis, favoring prolonged and heterogeneous repolarization and multiple re-entry circuits. The proposed link to sudden cardiac death is plausible but has not been demonstrated by our data.

Table 1

Comparison between human HFpEF and Dahl salt-sensitive rat model of HFpEF

	Human HFpEF	Rat HFpEF
Hemodynamic abnormality	+	+
Echocardiographic diastolic dysfunction	+	+
QTc prolongation	+	+
High sudden death rate	+	+
Increased fibrosis	+	+
Elevated baseline heart rate	+	−
Co-morbidities		
Hypertension	+	+
Diabetes Mellitus	+	−
Obesity	+	−
Old age	+	−